Can a simple Numerical Model Help to Fine-Tune the Analysis of Ground-Penetrating Radar Data? Hochebenkar Rock Glacier as a Case Study

Authors: Hartl, Lea, Fischer, Andrea, Klug, Christoph, and Nicholson, Lindsey

Source: Arctic, Antarctic, and Alpine Research, 48(2) : 377-393

Published By: Institute of Arctic and Alpine Research (INSTAAR), University of Colorado

URL: https://doi.org/10.1657/AAAR0014-081

Arctic, Antarctic, and Alpine Research, Vol. 48, No. 2, 2016, pp. 377–393
DOI: http://dx.doi.org/10.1657/AAAR0014-081

Can a simple numerical model help to fine-tune the analysis of ground-penetrating radar data? Hochebenkar rock glacier as a case study

Lea Hartl[1,2,*], Andrea Fischer[1], Christoph Klug[2], and Lindsey Nicholson[3]

[1]Institute for Interdisciplinary Mountain Research, Austrian Academy of Sciences, Technikerstr. 21a, ICT, 6020 Innsbruck, Austria
[2]Institute of Geography, University of Innsbruck, Innrain 52f, 6020 Innsbruck, Austria
[3]Institute of Atmospheric and Cryospheric Sciences, University of Innsbruck, Innrain 52f, 6020 Innsbruck, Austria (until May 2015 known as the Institute of Meteorology and Geophysics, University of Innsbruck, Austria)
[*]Corresponding author's email: Lea.Hartl@student.uibk.ac.at

ABSTRACT

Little is known about the thickness of active Alpine rock glaciers, yet they are important components of the local hydrology. We use GPR data to determine the depth of the bedrock of Äußeres Hochebenkar rock glacier (Austria). There is no detailed information available regarding density and composition of the rock glacier, and assumptions about the signal propagation velocity have to be made when processing the GPR data. We use a simple creep model based on surface displacement and slope to calculate the thickness of the rock glacier along a flow line. We calculated bedrock profiles along the flow line for three different time periods, using input from multitemporal digital elevation models. We improved the fit of the profiles by calibrating the values used for layer densities and considered the model valid where the modelled bedrock profiles are within error of each other. We then compared the modeled values with the GPR data to check whether our assumptions for the propagation velocity produced results that match the model. While the fit is good at the lower end of the rock glacier, the GPR data appear to overestimate depth in the upper region. We adjusted the propagation velocity accordingly and find maximum thicknesses of over 50 m and a mean thickness of 30–40 m. The insights gained from the modeling approach thereby improved the fine-tuning of the GPR analysis.

Introduction

Permafrost covers 24% of the land surface of the northern hemisphere (Lemke et al., 2007). Changes in depth and distribution of permafrost are triggered by climate change (Haeberli et al., 2011; Vaughan et al., 2013) and can have far-reaching effects on the local and regional hydrology (Cheng and Wu, 2007). Despite the large area of permafrost and its known susceptibility to climate change, there are few long-term data on changes and processes in frozen ground.

Rock glaciers are an example of an ice-rich form of mountain permafrost found in all mountain regions of the world, yet the volume of water stored in them, and the rates and controls on their flow and ice mass change, are generally poorly constrained (Roer, 2005; Haeberli et al., 2006). This is of concern in areas such as the arid and semi-arid Andes, where rock glaciers are a primary source of water (Brenning, 2008; Angillieri and Yanina, 2009), and in the Tian Shan, where they are expected to play an increasing role in local water resources under ongoing climate change (Bolch and Marchenko, 2009).

The number and size of rock glaciers in the Alps are small compared to these areas of concern; a few decades ago Barsch (1977) estimated that 0.03 km^3 of water was stored in rock glaciers per 1000 m^2 over the Swiss Alps, which is an order of magnitude less than in the Andes (Brenning, 2005). However, there is a long history of interdisciplinary studies of rock glaciers in the Alps (Haeberli et al., 2011; Springman et al., 2012). Two of the longest records of rock glacier surface velocity measurements, starting in 1918 and 1938, respectively, are from the Val Sassa rock glacier in Switzerland (Chaix, 1923; Barsch, 1996) and Äußeres Hochebenkar in Austria (Pillewizer, 1957; Vietoris, 1958, 1972; Schneider, 1999; Schneider and Schneider, 2001). Multiannual surface displacement data derived from aerial photographs are available for Murtèl rock glacier going back to 1932 (Barsch and Hell, 1975). More recently, movement of Alpine rock glaciers has been monitored by remote sensing at increasingly high resolution and accuracy, using digital photogrammetry (Roer and Nyenhuis, 2007; Kääb et al., 1998; Kääb et al., 2002) and airborne and terrestrial laser scanning (Kääb et al., 2003; Bollmann et al., 2012; Klug et al., 2012). While detailed geophysical data on rock glacier volume and composition are challenging and labor intensive to collect, the availability of both historical and increasingly high-quality modern-day information on rock glacier surface velocities allows estimates of other rock glacier properties from surface velocity, if appropriate relationships can be established. The relative abundance of data means that rock glaciers in the Alps can serve as a valuable testing ground for understanding rock glacier behavior and developing methodologies for monitoring and understanding their change that can then be exported to less data-rich regions, where the rock glacier water resource is of greater relevance to local ecosystems and societies.

In the Tyrol region of Austria, rock glaciers cover a total area of 167 km^2 (Krainer and Ribis, 2012). Äußeres Hochebenkar rock glacier (HEK) is an active tongue-shaped rock glacier in a northwest-facing cirque in the Ötztal Alps (Fig. 1). It covers an area of 0.47 km^2 and extends from a maximum altitude of 2830 m a.s.l. down to about 2360 m a.s.l., making it one of the largest active rock glaciers in the Tyrolean Alps. The rock glacier has two pronounced lobes, the larger one, on the orographic left side, showing significantly higher activity (Schneider and Schneider, 2001). Geologically the bedrock belongs to the Ötztal-Stubai complex and is composed mainly of paragneiss and mica schist. The mountain climate of the inner Ötztal is relatively dry. For the period 1971–2000, a mean yearly precipitation of 820 mm and mean annual air temperature of 2.2 °C was measured in Obergurgl (1938 m a.s.l.). The geomorphology, the climatological setting and the history of research at HEK are summarized in Haeberli and Patzelt (1982), Nickus et al. (2015), and Schallhart and Erschbamer (2015).

The ice content of HEK has been estimated at 50% of the rock glacier volume (Haeberli and Patzelt, 1982) in keeping with more recent studies at other Alpine rock glaciers (Hausmann et al., 2007, 2012), and the rock glacier is thought to have a massive ice core (Nickus et al., 2015). Surface flow velocities have been monitored continuously since 1938 by measuring the displacement of marked rocks along three to four cross profiles (Fig. 1) (Pillewizer, 1957; Vietoris, 1958, 1972; Schneider and Schneider, 2001). Surface velocities at HEK are high compared to many other rock glaciers and values of over 3 m a^{-1} have been measured. In the past decade, surface velocities between approximately 1 and 2.5 m a^{-1} were observed. From the mid-1990s to 2004, the rock glacier accelerated significantly. After 2004, the trend in velocity becomes less clear and acceleration paused for several years. Nickus et al. (2015) suggested that the exceptionally warm summer of 2003 caused changes in the flow of the rock glacier due to ice loss. In recent years, up to 2015, velocities have increased again. Extensive monitoring of the lower parts of the rock glacier carried out by means of terrestrial photogrammetry has found horizontal surface displacement of a similar magnitude as that determined by the geodetic measurements (Kaufmann and Ladstätter, 2002a, 2002b; Kaufmann, 2012; Ladstätter and Kaufmann, 2005). Recently, Klug et al. (2012) and Bollmann et al. (2012) investigated the spatial distribution of horizontal and vertical surface displacement using repeat airborne laser scanning (ALS) data, which can reveal high-resolution spatial patterns of both surface lowering and horizontal displacement, as well as digital elevation models (DEMs) derived from orthoimages. These investi-

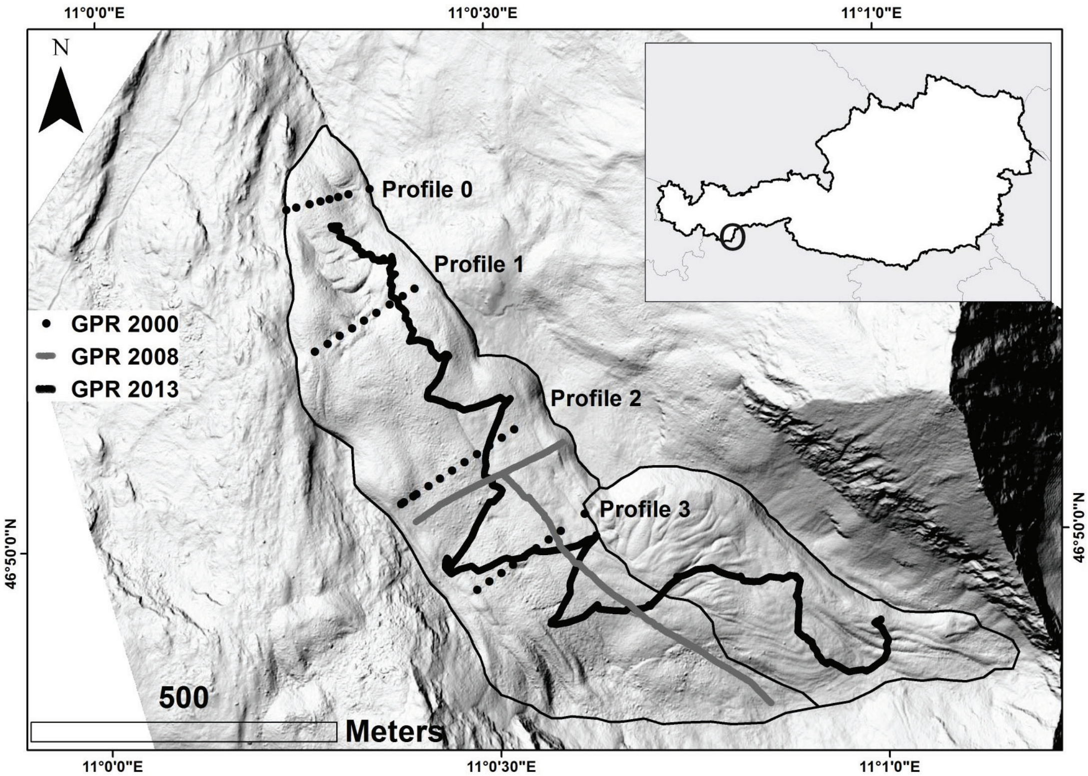

FIGURE 1. Location of Äußeres Hochebenkar (HEK) rock glacier in the Ötztal Alps, Austria. Ground-penetrating radar (GPR) data points and profiles collected in 2000, 2008, and 2013, as well as the outlines of the two lobes of the rock glacier are shown on a hillshade image based on a 2009 LiDAR digital elevation model (DEM).

gations reveal that vertical changes are small in the upper part of the rock glacier, while the terminus is thinning and extending.

Ground penetrating radar (GPR) is a useful tool for determining rock glacier thickness, as well as internal structure. However, data quality can vary considerably and interpretation can be difficult if no further information, such as borehole data or additional supplementary geophysical data, on composition and density is available (Hauck and Kneisel, 2008).

The aims of this study are to (1) analyse GPR data collected at HEK rock glacier, discussing assumptions made in the interpretation of the data, and (2) examine the utility of a simple flow model based on input from multitemporal surface terrain models in verifying these assumptions. We estimated the thickness of the rock glacier from the GPR data, based on estimates of signal velocity and rock glacier composition. The creep model calculated thickness based on surface velocity and slope angle derived from DEMs. Using velocity and slope input from different years, we computed bedrock profiles for three time steps. We calibrated the model parameters by varying layer densities within an expected range to improve the fit of the profiles, based on the idea that they should remain the same over time (i.e., within an expected margin of error). Assuming the model works as desired, model results can be compared to the bedrock depths found by GPR to evaluate and adjust the initial assumptions made in the interpretation of the GPR.

Methods and Data

Digital Elevation Models

Digital elevation models (DEMs) of Hochebenkar rock glacier for the years 1953, 1969, 1990, 1997, 2009, and 2010 were used to analyze surface displacements of HEK over the past six decades. The 1953, 1969, 1990, and 1997 DEMs were generated from gray-scale aerial photographs with the required calibration reports. Image orientation, automatic DEM, and digital orthophoto generation were performed within the application OrthoEngine of the Geomatica software (version 10.3). For a detailed description of the applied photogrammetric methods, see Baltsavias et al. (2001), Kääb (2010), and Klug et al. (2012). The DEMs were generated automatically from mono-temporal stereo-models with 1 m spacing and the orthoimages were calculated with 0.2 m ground resolution. The 2009 and 2010 DEMs were compiled from ALS data with a spatial resolution of 1 m and a minimum mean point sampling density of 3.5 points per meter (Bollmann et al., 2012). A comparison between the ALS DEMs of HEK and the dGNSS (differential global navigation satellite system) heights at 11 fixed points returned a root-mean-square error (RMSE) of 0.09 m in 2009, and a slightly worse RMSE (0.11 m) in 2010.

Accordingly, the accuracy of the older DEMs derived from photogrammetry was assessed by comparing each DEM with the high-quality DEM of the ALS flight campaign of 2009. Three areas of stable ground with comparable surface structure (slope, aspect, height) to the rock glacier were identified for the DEM intercomparison. The calculated RMSE was less than 0.6 m (Table 1). This indicates that vertical accuracy of all DEM heights is better than 0.6 m (Klug et al., 2012).

Horizontal Displacements

Block movement at four cross profiles is monitored annually by geodetic surveying. Velocities of single blocks are available for 1953–1955, 1981–1985, and since 1997. For the other periods, only the mean velocity at each profile is known. Additionally, horizontal surface displacement has been calculated for certain time frames using the image correlation software Imcorr (Scambos et al., 1992). Imcorr has already been applied to calculate flow velocities of glaciers using a variety of input data acquired from aircraft or satellites (Dowdeswell and Benham, 2003). The software identifies displacement rates as a function of systematic changes in image digital numbers. Detailed information about this software is given in Bollmann et al. (2012). In this study, 39 dGNSS measurements of the annual geodetic measurement campaign were used for validation of the 2009–2010 data (Fig. 2, Table 2). Comparisons between the ALS-based surface displacement raster and dGNSS data indicate an accuracy (standard deviation) of the calculated displacement rates of 0.3 m for the period 2009–2010.

TABLE 1

Calculated root-mean-square error (RMSE) for the generated digital elevation models (DEMs) versus the 2009 airborne laser scanning (ALS) DEM.

DEM	RMSE (stable areas/fixed points) (m)
2010 (ALS)	0.11/0.09
2009 (ALS)	Ref./0.09
1997	0.41
1990	0.42
1969	0.29
1953	0.58

GPR

GPR is widely used to determine the structure and ice content of rock glaciers (Arcone et al., 1998; Maurer and Hauck, 2007; Hauck and Kneisel, 2008, Von der Mühl et al., 2002). While penetration depth increases at low frequencies, the depth resolution decreases. Frequencies between 6.4 and 250 MHz have been used to measure thickness of up to about 40 m and internal properties of rock glaciers in the Alps, the polar regions, and the United States (Fukui et al., 2007; Degenhardt, 2009; Degenhardt et al., 2003; Nickus et al., 2015).

HEK has been surveyed with two different radar systems, in 2000 (by Nickus et al., 2015), 2008, and 2013 (this study) (Fig. 1). During the first GPR campaign in 2000, a transmitter with a frequency of 6.4 MHz (Narod and Clark, 1994; Nickus et al., 2015) was used. The signal was displayed on a digital 100 MHz Scopemeter. Data points were taken along three cross-profiles that are also used for the annual geodetic displacement measurements. Bedrock depths between 31 m and 43 m were found at profile 1, between 32 m and 50 m at profile 2, and between 33 m and 58 m at profile 3, using an estimated propagation velocity of 0.155 m ns^{-1}. At the lowest profile (profile 0), it was not possible to obtain an interpretable GPR signal with the instrumentation used. Instead, maximum depths of about 15 m were found by comparing a recent DEM with topographic information from 1953,

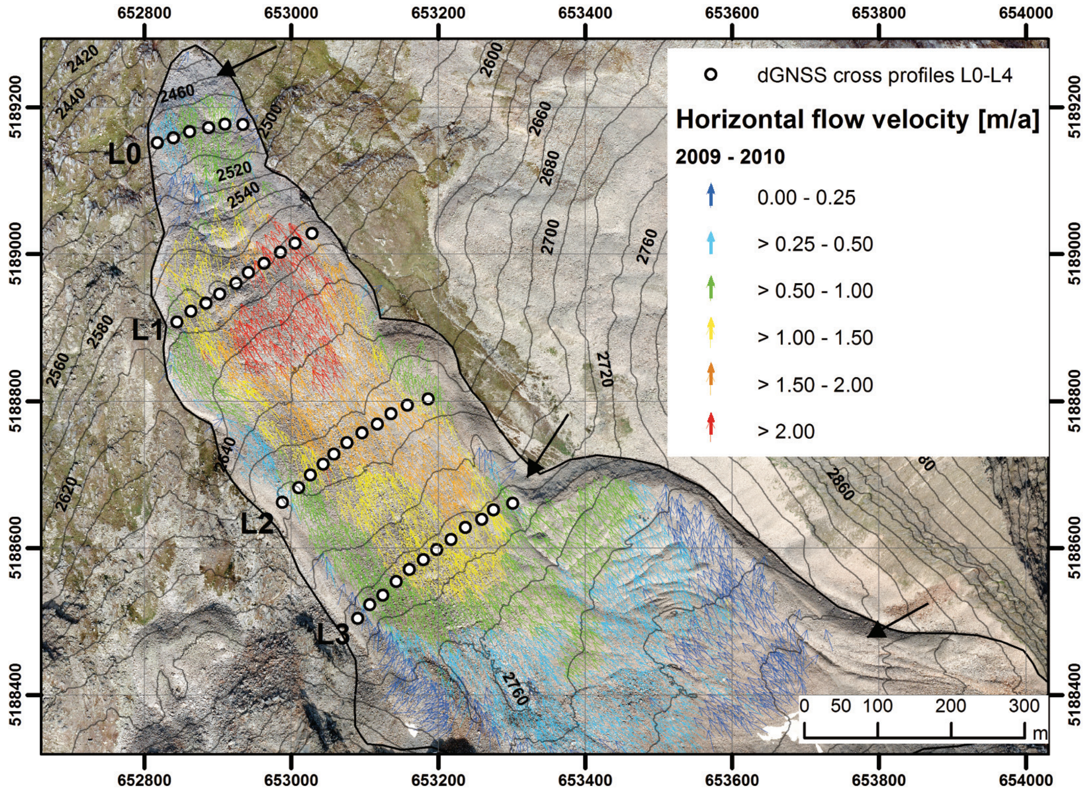

FIGURE 2. Annual surface velocity of HEK rock glacier for 2009–2010, accurate to 0.3 m, based on ALS DEMs from 2009 and 2010, results from Imcorr output. L0 to L3 indicate location of dGNSS measurement points along four cross profiles. Black arrows indicate areas with artefacts and bad correlation.

when the rock glacier terminated above this lowest profile. Rock glacier thickness is greatest at the center and decreases toward the margins. The bedrock could not be measured with GPR at this line because of the GPR configuration used and the shallowness of the layer. More detail on methods and results of this GPR campaign can be found in Nickus et al. (2015).

For the latter two surveys, a GPR system manufactured by GSSI (http://www.geophysical.com/gssibrochures.htm), a SIR 3000 recorder, and 3200 MLF antennas operating at 15 MHz were used. The frequency was chosen in order to allow for the detection of the bedrock reflector, as well as potentially gaining information about the thickness of the ice-free surface debris, which could not be detected with the lower frequency used in the 2000 campaign. The measurements were carried out in winter, and the GPR system was mounted on a sled construction, allowing for easier movement. The GPR data gathered in 2008 and 2013 were processed using the ReflexW software, version 6.0.9, to apply a static correction and automatic gain control, as well as filter operations for noise reduction. In 2008, a longitudinal profile was measured roughly in the orographic center of the

TABLE 2

Comparison of adjusted horizontal displacement rates from Imcorr and dGNSS (Imcorr–dGNSS), 2009–2010, *n* = 39.

Imcorr–dGNSS	Mean (m)	Amean (m)	Std (m)	Max (m)	Min (m)	RMS (m)	R^2
Pts. 09/10	–0.10	0.25	0.36	0.96	–1.28	0.37	0.92

Notes: Mean = mean deviation between dGNSS and Imcorr; Amean = average absolute deviation; Std = standard deviation; Max/Min = maximum/minimum deviation; RMS = root-mean-square error; R^2 = coefficient of determination.

rock glacier between 2690 m a.s.l. and 2810 m a.s.l. This profile consists of 281 data points and is 580 m long. A 275-m-long transect of 303 data points was taken near profile 2, at 2690 m a.s.l. A third profile showed no identifiable reflectors and was discarded. In 2013 a total of 15,269 data points were gathered along a 2210-m-long track. The data points were plotted along GPS tracks taken during the field campaigns.

For the survey in 2000, Nickus et al. (2015) assumed a propagation velocity of 0.155 m ns^{-1}, referring to previously published values used in other studies (Hausmann et al., 2007; Hauck and Kneisel, 2008). However, propagation velocity was not measured and may vary significantly in time and space with changes in grain size, porosity, and ice content. For example, Hausmann et al. (2012) found densities between 1410 and 2150 kg m^{-3} at Ölgrube and Kaiserberg rock glaciers, using gravimetry measurements, and it is assumed in this study that similar variations may occur at HEK. If the density of ice is 900 kg m^{-3} and the density of debris is roughly that of granite (~2700 kg m^{-3}), a ratio of 1:3 of debris to ice results in an overall density of 1350 kg m^{-3}, whereas a ratio of 3:1 would yield an overall density of 2250 kg m^{-3}. The propagation velocity of a radar pulse in granite is 0.130 m ns^{-1} (Davis and Annan, 1989), while values for ice range from 0.167 to 0.169 m ns^{-1} (Kovacs et al., 1995; Bauder et al., 2003; Glen and Paren, 1975).

In this study, to account for velocity variations due to changes in density, composition, and air content, depth was calculated for a minimum "likely" propagation velocity of 0.140 m ns^{-1} (~25% ice content) and a maximum velocity of 0.160 m ns^{-1} (~75% ice content). As travel time increases, the uncertainty in depth due to the potential velocity range increases. While different propagation velocities could be used for different identified layers in the subsurface (ice-rich permafrost, ice-free debris, snow), this was not done because it would prevent intercomparability of surveys across all measurement dates, as no information about layering was available from the 2000 GPR campaign. On average the spread of derived thickness obtained using the velocities given above results in an uncertainty of 10%–12%. For our initial evaluation of the 2008 and 2013 GPR data, we used a propagation velocity of 0.155 m ns^{-1} in keeping with Nickus et al. (2015).

The rock glacier was snow-covered during the 2008 and 2013 measurements. Probing snow depth on the rock glacier in a representative manner is very difficult, as local snow thickness varies greatly (by a meter and more) due to the highly uneven surface of large blocks. Assuming a propagation velocity of 0.290 m ns^{-1} in dry snow (Span et al., 2005), the radar pulse travels through 2 m of snow in 6.9 ns (probing next to the rock glacier in 2013 yielded snow depths in this range). Doubling that to account for the return journey gives a travel time in snow of about 14 ns, which amounts to 3.5% of a typical total run time of 400 ns over a specified 30 m thickness. The error from snow is more significant in thinner regions of the rock glacier and less so in the thicker parts, unlike the error caused by velocity variations from rock glacier layering. To account for the likely impact of variations in snow cover, density, and composition of the rock glacier on the propagation velocity of the radar pulse, an uncertainty of ±15% was assumed for all derived thicknesses for 2008 and 2013.

Creep Modeling

The basal shear stress of an idealized glacier can be written as

$$\tau_b = \rho * g * H_i * \sin(\alpha) \qquad (1)$$

where ρ = density, g = acceleration of gravity, H_i = thickness of the ice, α = the slope angle at the surface, and it is assumed that τ_b equals the driving stress τ_d (form factor ~1) (Cuffey and Paterson, 2010).

Surface velocity can be expressed as

$$V_s = V_b + \frac{2A}{n+1} * \tau_b{}^n * H_i \qquad (2)$$

where V_b is the velocity at the base, and A and n are the appropriate constants of Glen's flow law (Glen, 1958).

Assuming no basal sliding takes place, it follows that the glacier thickness can be expressed as

$$H_i = \left(\frac{V_s(n+1)}{2A(\rho g sin(\alpha))^n} \right)^{\frac{1}{n+1}} \quad (3)$$

Konrad et al. (1999) modified this equation to include the effect of a layer of ice-free surface debris on a rock glacier, so that

$$H_r = \left(\frac{V_s(n+1)}{2A(\rho g sin(\alpha))^n} + \frac{\rho_d}{\rho_i} d^{n+1} \right)^{\frac{1}{n+1}} - \frac{\rho_d}{\rho_i} d \quad (4)$$

where H_r is the thickness of the deforming, ice-rich layer; ρ_i is the density of this layer; ρ_d is the density of the debris, and d is the average thickness of the debris. Combining H_r and d gives the modeled rock glacier thickness.

We apply this equation to a central flow line of the rock glacier for different time periods using input derived from the available multiannual DEMs in order to provide an alternative data set of the glacier thickness. The calculated thicknesses yield a modeled bedrock profile along the flow line. Surface velocities and slope angles change with time, but for the model to be considered valid, the position of the bedrock profile must remain the same or within the margin of error associated with the model uncertainty, regardless of changing surface velocity and slope input. Comparison of the modeled bedrock profiles at each modeled date was used to evaluate the model performance. The required model inputs are surface velocity and slope angle, the thickness of the surface debris layer, density of the layers, and the flow law constants n and A.

Surface slope angle and velocity are derived from the DEMs. The surface of the rock glacier is marked by strong, small-scale variations in the form of ridges, furrows, and crevasses, which are well represented in the high-resolution ALS DEMs (Klug et al., 2012). In order to avoid these surface features affecting the thickness calculations, slope angles and velocity data points were resampled as averages over 25 m cells.

The thickness of the surface debris layer was identified from the higher frequency GPR measurements of 2008 and 2013, and we used an average value from both years to increase the available data, as GPR data for the surface debris thickness along the flow line was only sampled where the GPR tracks intersect the flow line. At these intersections, the GPR data indicated surface debris thicknesses within 1 m of the mean of all data points. In the modeled rock glacier thickness, a change in thickness of 1 m of the surface debris layer leads to a change of no more than 5% in total thickness on average.

A was taken to be 2.4×10^{-24} Pa^{-n} s^{-1}, in keeping with Konrad et al. (1999). This is the value suggested for ice at −2 °C (Cuffey and Paterson, 2010). Changing A by ±30% results in a change in modeled mean rock glacier thickness of up to about 2 m (7%–10%). As deformation in the ice-rich layer arises from ice deformation, n is taken to be 3, which is widely used for the viscoplastic deformation suitable for glaciological applications (e.g., Cuffey and Paterson, 2010).

For an estimate of the density of the ice-rich permafrost layer and the ice-free debris layer, we refer to values determined by Hausmann et al. (2012) at Ölgrube and Kaserberg rock glaciers, that is, a debris density of 1604–1900 kg m^{-3} and a density of 1410–2150 kg m^{-3} for the ice-rich layer. Density variations within these values (Hausmann et al., 2012) can cause changes in modeled thickness of up to around 3 m.

We discuss how and if the differences between the modeled bedrock profiles can be reduced by calibrating the values used for layer densities and debris thickness. The densities of the ice-rich permafrost and debris layers are varied within the range found by Hausmann et al. (2012). Layer densities should remain the same over time, as large changes are considered unlikely. The thickness of the debris layer and, in consequence, the overall density are allowed to change slightly over time. Agreement is considered good when the mean and maximum differences between the bedrock profiles are small.

This process of calibration was carried out for a 100-m-long stretch of the flow line located in the upper region of the rock glacier at roughly 2720–2755 m. The rock glacier surface has not undergone any substantial changes in this section along the time line and is of fairly uniform incline.

Assuming the creep model works as desired, the model is expected to provide bedrock profiles that are consistent over time. Bedrock depth along a central flow line was modeled using surface velocities and slope angles from three different time periods (1953–1969, 1990–1997, 2009–2010). Assuming the errors on the model input parameters to be independent and summing them in quadrature provides an error assessment of about 15% of the mean modeled thickness along the flow line for all three time periods. The modeled bedrock profiles are considered consistent if they are within this error of each other.

Given the uncertainty of the initial assumption of the propagation velocity interpretation of the GPR data, comparison of the modeled rock glacier thickness with those derived from the GPR can be used to provide an independent check on the GPR-derived thicknesses. If the initial assumptions made in the interpretation of the GPR are wrong, model results are expected to differ strongly from the GPR results and the propagation velocity could be adjusted accordingly and calibrated using the modeled thickness.

Results

Creep Modeling

To assess quantitative agreement and adjust parameters, a calibration process was carried out for a section of the flow line taken as representative (Fig. 3). The best fit of the three bedrock profiles was achieved with a low density for the debris layer (1604 kg m^{-3}) and a high density for the ice-rich layer (2150 kg m^{-3}). With these values the mean (maximum) difference between the modeled profiles for the section of the flow line used for calibration was –0.5 m (3 m), 5 m (9 m), and 6 m (7 m) for the periods 1953–1969 vs. 1990–1997, 1953–1969 vs. 2009–2010, and 1990–1997 vs. 2009–2010, respectively. For the entire flow line, the mean differences were between –0.3 and 2 m, while the maximum differences ranged from 9 to 11 m.

The surface velocity of the rock glacier has increased significantly over the majority of the flow line from 1997 to 2010, including in the section used for calibration. There are no signs to suggest an increased amount of debris input, so it can be assumed that more debris is transported downhill as the velocity increases, resulting in a thinning debris layer (Ikeda, 2004; Olyphant, 1987).

The fit was improved further by reducing the thickness of the debris layer from 11 m (mean thickness from the initial GPR analysis) to 9 m for the most recent period. To account for this in the overall density value, the density ratio between the debris layer and the ice-rich layer was changed

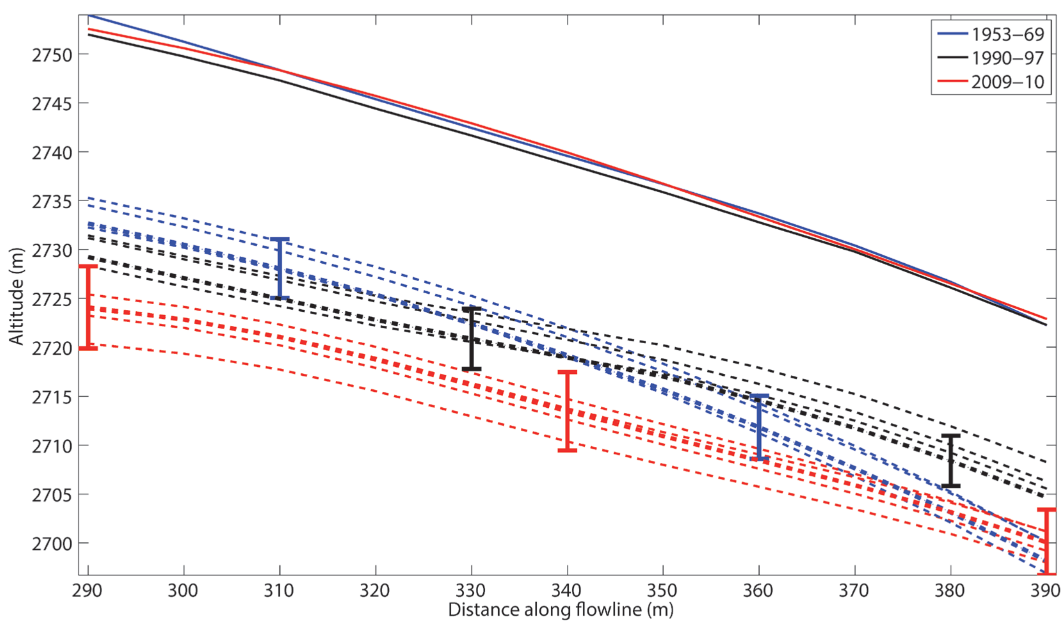

FIGURE 3. A 100-m-long section of the flow line that was used to improve the model fit by calibrating the layer densities and thickness of the debris layer. The thick dashed lines with error bars show the best fit that was achieved within the limit values and under the conditions that densities remain the same for the three time steps. The thinner dashed lines indicate the potential spread due to varying the parameter values. The solid lines show the surface elevation as derived from the 1969, 1997, and 2010 DEMs.

from 25%:75% to 20%:80% for this period. For the calibration section of the flow line, we found a mean (maximum) difference of 4 m (9 m) and 5 m (6 m) for the periods 1953–1969 vs. 2009–2010 and 1990–1997 vs. 2009–2010, respectively. For the entire flow line, the differences decrease by a similar magnitude.

The modeled bedrock profiles lie within the expected range of uncertainty throughout the flow line. Varying the layer densities within the limit values mentioned above yields changes in the mean and maximum differences that are relatively small compared to the general uncertainty. Qualitatively, the modeled bedrock profiles generally show better agreement in regions where the rock glacier is thinner (Fig. 4).

Differences in the modeled bedrock cannot clearly be attributed to corresponding velocity differences. In the lowest section of the rock glacier, surface elevation has decreased since 1969, while the terminus has moved farther downhill. There are some large discrepancies between the oldest profile and the two more recent ones here (Fig. 4).

GPR

The GPR data gathered in 2008 and 2013 indicated two main reflectors below the rock glacier surface, which we interpreted as the interface between surface debris and the ice-rich permafrost, and the permafrost-bedrock interface, respectively.

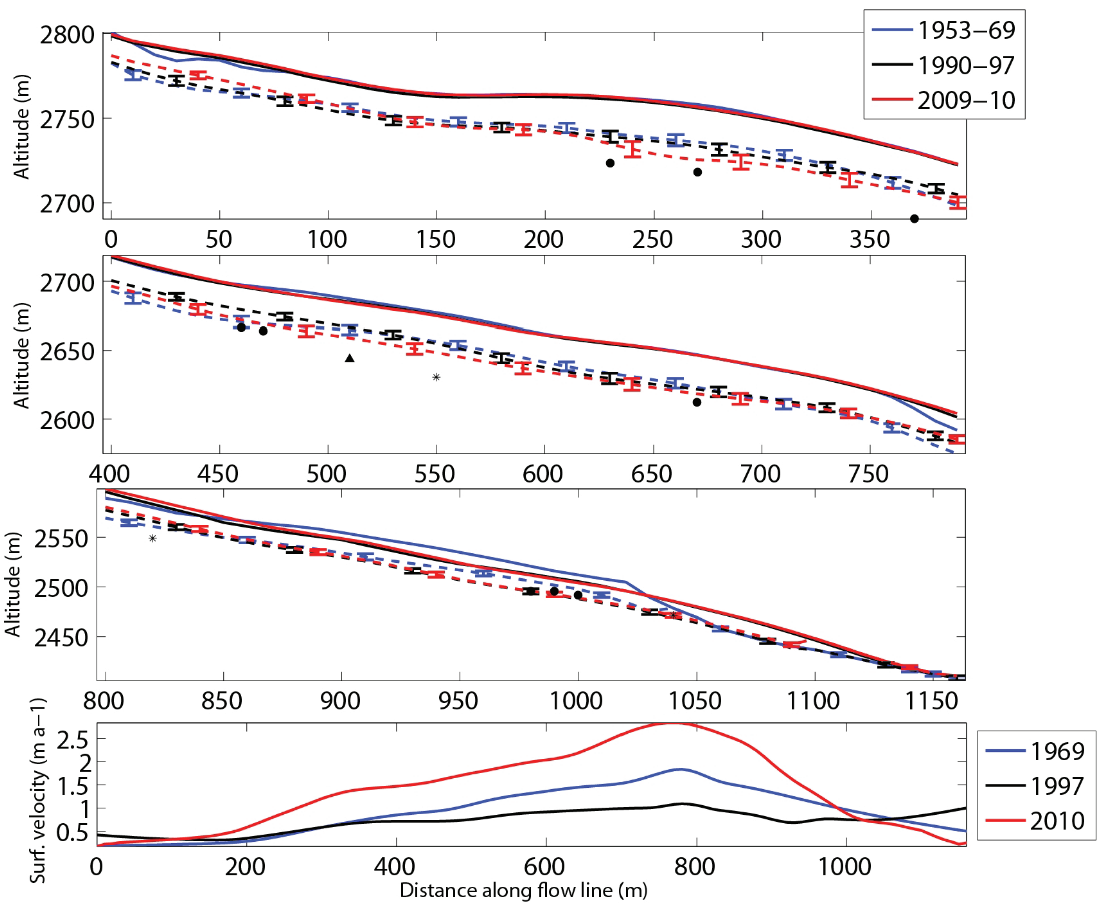

FIGURE 4. The upper three panels show consecutive sections of the flow line. Solid lines show the surface of the rock glacier in three different years. Where the GPR profiles intersect the flow line, the depth of the bedrock as determined by the GPR at a propagation velocity of 0.155 m ns^{-1} is marked. Circles show GPR values from the 2013 measurement campaign, stars the values from 2000, and triangles the values from 2008. The bedrock depth was modeled using velocities extracted from DEMs for the periods 1953–1969, 1990–1997 and 2009–2010, as well as the respective surface slopes (dashed lines). The lowest panel shows the surface velocities in m a^{-1} along the entire flow line during the respective time periods, as extracted from the DEMs.

TABLE 3

Depth of bedrock and the ice-free surface debris, as measured by ground-penetrating radar (GPR) in 2000, 2008, and 2013, using signal propagation velocities from 0.14 to 0.16 m ns^{-1} to account for uncertainties regarding the composition of the rock glacier.

Propagation velocity	Average depth of surface debris (m)		Average depth of bedrock (m)		
(m ns^{-1})	2008	2013	2000	2008	2013
0.140	6.8	9.9	33.6	39.0	32.0
0.155	7.8	11.2	35.0	43.9	35.6
0.160	8.1	11.6	39.0	44.9	36.8

These two layers can be seen above the terrain step at 2580 m a.s.l. Below the step, only one clear reflector remains. In the radar data showing two reflectors, the upper layer boundary can generally be seen fairly well, while the bedrock reflector is often hard to detect with confidence and can generally not be identified for each entire profile (Fig. 5).

The maximum difference in total thickness of the rock glacier for the minimum and maximum velocity was roughly 7 m at a travel time of 691 ns, which corresponds to a thickness between 48 m and 55 m. The average total thickness over all measurements was 33 m for 0.14 m ns^{-1} propagation velocity and 40 m for 0.16 m ns^{-1} propagation velocity. Table 3 shows the average thickness over the velocity spread for the years 2008 and 2013, as well as the thickness calculated with a velocity of 0.155 m ns^{-1} for comparability with the 2000 data. It should be noted that the values for the different years cannot be compared directly, as the GPR data were taken in different parts of the rock glacier.

The 2013 data revealed that bedrock depth decreased markedly below around 2600 m, where the terrain steepens. The 2013 data intersect the 2000 data here and indicate that thickness may have decreased significantly in this zone. Comparing DEMs from different years, Klug et al. (2012) found negative vertical changes between 1 and 4 m in this area between 1997 and 2009. Up to an altitude of about 2675 m a.s.l. (Profile 2), the GPR results indicate that the rock glacier is thickest in the center and thins toward the margins. Above this altitude, maximum thickness appears to shift toward the orographic left margin. The terrain beside the rock glacier gradually steepens into a cliff face here, so a depression of the bed seems possible.

Where the GPR tracks cross the central flow line used for the creep model or pass with 10 m of it, the measured bedrock depths were compared to the modeled depths. Using the "initial guess" propagation velocity of 0.155 m ns^{-1} and the "best fit" model parameters, the GPR generally appeared to overestimate depth compared to the modeling approach in the upper regions of the rock glacier, while agreement between GPR and model was good below about 2500 m a.s.l. where thickness is lower and the GPR signals are of better quality.

In our final assessment of the GPR data, we therefore used the lower limit of what we consider a likely propagation velocity (0.140 m ns^{-1}) for measurements taken above 2500 m. The GPR values lie within the expected range of error after reprocessing. Nonetheless, differences between the GPR and model remain, in some sections of the flow line, more so than in others.

The resultant rock glacier thickness shows maximum depths in excess of 50 m in the upper regions of the rock glacier, while it thins rapidly in the steeper regions of the tongue. About 40% of the rock glacier area shows depths between 30 and 40 m. Greater depths occur only on the orographic left side above 2600 m a.s.l. The general pattern is in keeping with the earlier results from 2000 (Nickus et al., 2015). Due to the lower propagation velocity we used, thickness values are lower in the upper regions of the rock glacier. A rough approximation of the thickness distribution is shown in Figure 6.

Discussion

Creep Modeling

We acknowledge that a fundamental source of uncertainty is whether a creep law generally used for ice can be used to describe rock glacier movement. Haeberli and Patzelt (1982) suggested that

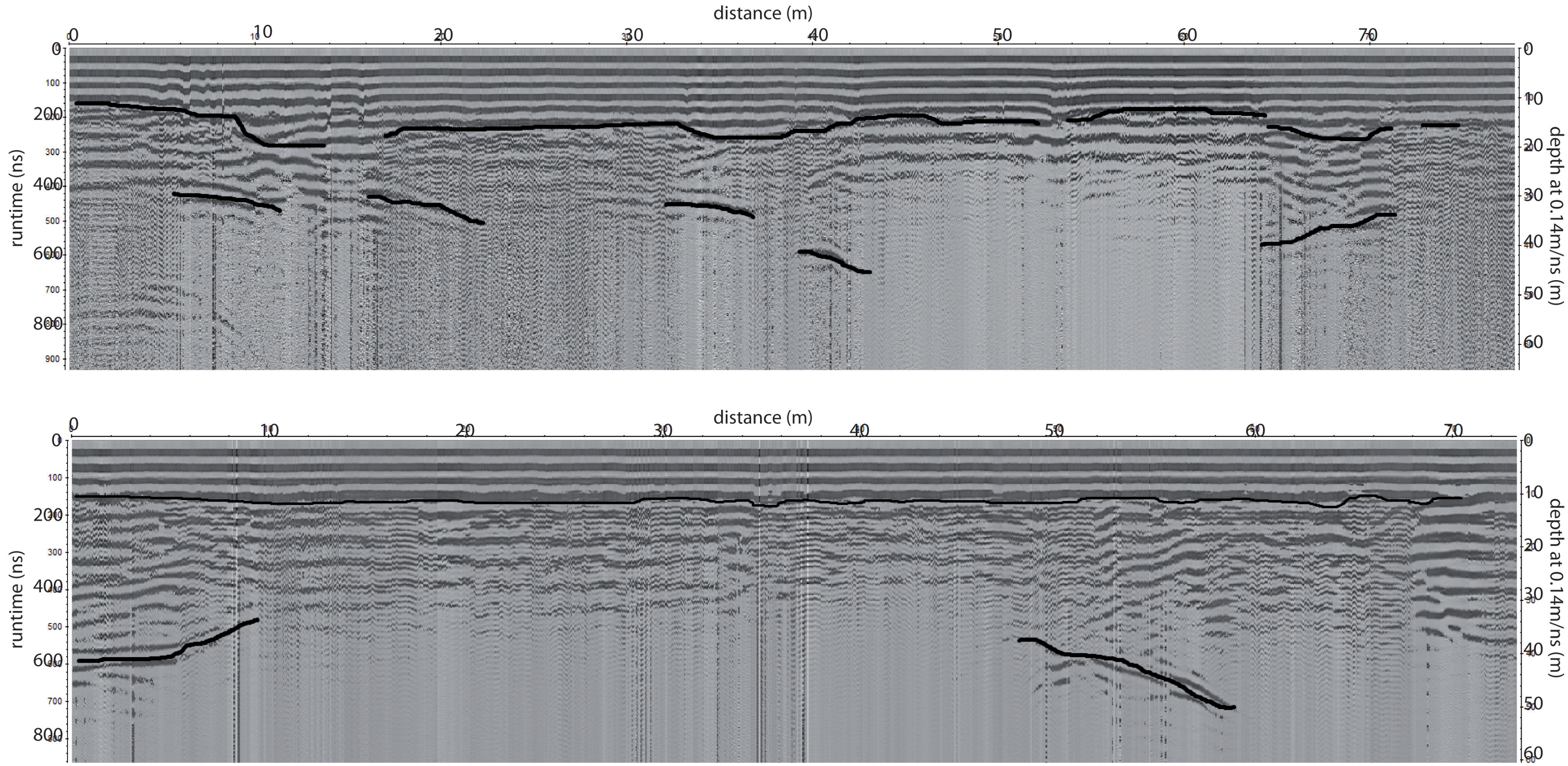

FIGURE 5. **Exemplary radargrams from the 2013 measurement campaign. The upper pannel shows a section at about 2625–2675 m, the lower panel shows a section at about 2700–2775 m. The upper and lower reflector are indicated where visible.**

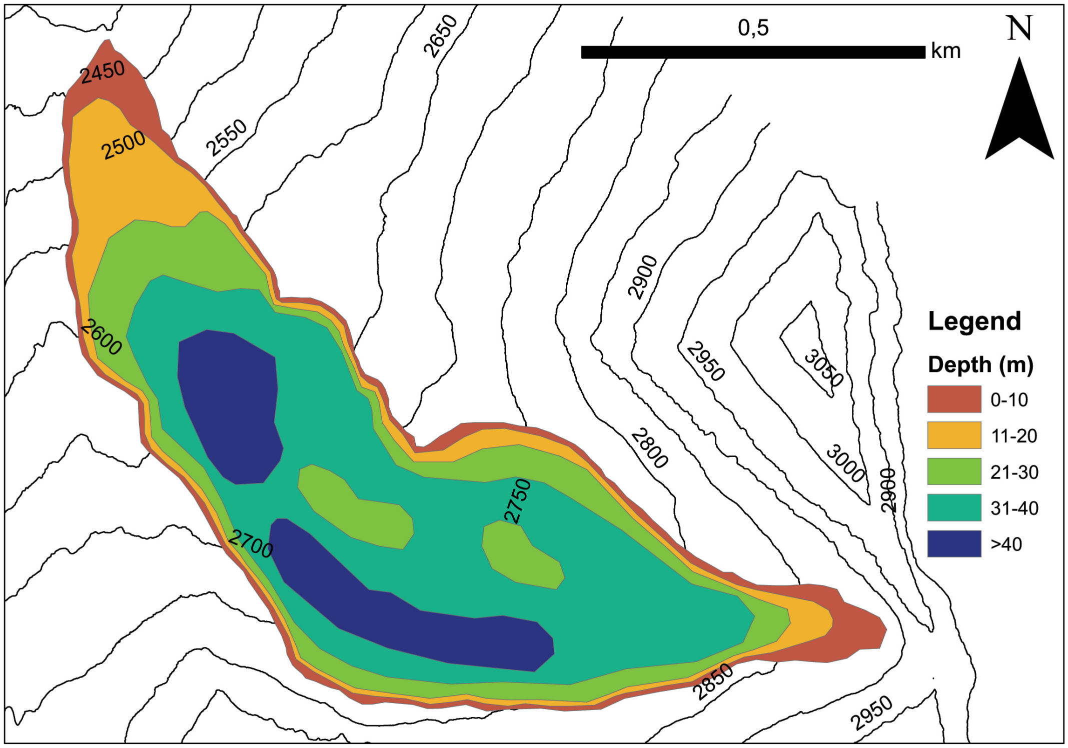

FIGURE 6. Approximate thickness distribution at Outer Hochebenkar rock glacier as estimated from the GPR data. The colors indicate the depth of the bedrock. The rock glacier thins rapidly toward the tongue. The thickest parts are located on the orographic left side of the rock glacier.

the movement of HEK rock glacier can mainly be attributed to the deformation of ice and therefore a stress regime similar to that of glaciers can be applied. Kääb et al. (1998) and Kääb and Vollmer (2000) stated that supersaturated permafrost can be approximated as behaving like massive ice due to incompressibility, while this may not be the case for structured permafrost. Rignot et al. (2002) found rock glacier motion similar to that of glaciers in Antarctica and discussed that the rheology of rock glaciers is comparable to that of glaciers in cases where massive ice is present. Haeberli et al. (2006) mentioned ice content exceeding saturation as a condition for applying ice rheology. Konrad et al. (1999) argued that the assumptions made in developing their modified version of Glen's flow law (which we used in this study) are backed by borehole data from Galena Creek and Murtél rock glaciers. We suggest that this is a valid best-guess approach, which should be improved upon in the future if better information regarding the composition of Hochebenkar rock glacier becomes available.

While it is likely that variations in air temperature are a main control for rock glacier acceleration or deceleration (Roer et al., 2005; Kääb et al., 2007), other factors, such as the presence of liquid water (Ikeda et al., 2008), a changing mass balance or basal sliding, should also be considered in future modeling of rock glacier dynamics. An appropriate discussion of these issues is beyond the scope of the presented study, which focuses on developing a very simple model that allows a first-order assessment of rock glacier thickness and the validation of assumptions made in the interpretation of GPR data due to limited available information on rock glacier composition.

The aim of our study was to develop a first-order estimate of rock glacier thickness from surface information that is easy to apply and does not require detailed information regarding composition. For this reason and because such data are not available to us, we did not vary layer densities or debris thickness along the length of the flow line. Doing so might well improve the model fit of the bedrock profiles for the different points in time. Varying the layer densities within the limit values suggests that the ice-rich permafrost layer of our two-layer model is on the dense end of the spectrum we consider likely, implying a fairly high percentage of debris within the layer, at least in the upper parts of the rock glacier.

The largest discrepancies between the three bedrock profiles occurred at the lower end of the flow line. Since 1969, the surface elevation of the rock glacier has decreased here, while the terminus has moved farther downhill. For the sake of simplicity and to be consistent in the logic of the approach, we used a mean value of debris thickness in the model (mean values for all parameters). In the terminus region, overall thickness approaches and dips below this value of debris thickness, which partially explains problems in this zone.

Although there are large uncertainties to the modeling approach, we suggest that the consistency within the error is a sign that it can be used for a rough approximation of rock glacier thickness. For us, this proved helpful in evaluating the GPR data.

GPR

At the locations where the GPR measurements from 2008 and 2013 intersect, thickness appears to have decreased in the time between the measurements. While this may in part indicate problems in the interpretation of the data, comparing DEMs from 2006, 2009, and 2011 confirmed a lowering of the surface in these areas by up to 2 m.

While the uncertainty in bedrock depth introduced by density and thus velocity variations is only 1–2 m at the comparatively thin tongue, it rises to values of 5–7 m in the thickest parts. The rock glacier is characterized by pronounced furrows and ridges, as well as crevasse-like formations, which shift in size and position from year to year. This can cause further errors when comparing GPR data from different years, particularly in the rapidly changing zone near the terminus.

The varying quality of the reflectors identified in the radargrams suggests that rock glacier depths of 40 m and more are near the upper limit of what can be measured with a GPR at 15 MHz. Nickus et al. (2015) did not report problems detecting bedrock reflectors using 6.4 MHz, yet upper reflectors cannot be detected with this frequency. In the 2008 and 2013 data, an upper reflector, probably indicating the interface between ice-free debris and ice-rich permafrost, could be detected well in the upper part of the glacier, yielding information on the ratio of ice-free debris to ice-rich permafrost. In the lower, thinner part of the rock glacier, only one reflector remained visible. An explanation could be that there is no layer separation in this part of the glacier. However, even with clear layer separation, it is likely that the vertical resolution of the GPR was insufficient to determine an upper reflector in this comparatively thin part of the rock glacier. For future GPR campaigns, joint multifrequency measurements would be desirable.

Can a Simple Numerical Model Help to Fine-Tune the Analysis of Ground Penetrating Radar Data?

Our simple numerical model was helpful for fine-tuning the GPR analysis. Comparing the GPR data with the modeled values suggested that the “initial guess” propagation velocity was too high in the upper regions of the rock glacier, while it fits the modeled data well at the tongue. This implies that propagation velocity varies considerably within the area of the rock glacier because of variations in density and composition. While the modeling approach proved useful for dealing with GPR data of varying quality, it naturally cannot replace more detailed geophysical measurements. Nonetheless, we see the results of the model as an indication that different propagation velocities should be applied in certain regions of the rock glacier and believe that doing so improved the quality of the GPR results, avoiding a systematic overestimation of the thickness. Model results also implied that a low propagation velocity should be used for most of the rock glacier, which in turn suggests that the ice content may be lower than previously thought. Considering the wider perspective and possible applications at other sites, we believe that our method can help to improve GPR analysis at comparable rock glaciers where boreholes or other geophysical data are not available or data quality is poor. A main assumption of our method is that we use a simple creep law to approximate rock glacier movement.

We have detailed our arguments for this above. If the method is to be applied at another site, it should be carefully considered whether or not this is a valid approach for the site.

Summary and Conclusions

In this study, we calculated rock glacier thickness using a simple creep model and compared model results with GPR data. GPR is a useful tool to investigate the thickness of midlatitude rock glaciers. However, depths ranging from a few meters to over 50 m, as found at Hochebenkar, require the frequency to be adjusted accordingly, which means that details are lost in the upper layers and/or that the bedrock horizon is not always clearly visible. In the absence of direct observations of rock glacier composition from a drilled borehole that could be used to constrain GPR velocities, various assumptions based on measurements from similar sites had to be made regarding the composition and density of the rock glacier for the interpretation of the GPR presented in this study.

The thickness of the rock glacier was modeled from surface velocity, slope angle, and surface debris layer thickness using a simple slab flow model. The model performance was cross-checked by applying the model to input extracted from multitemporal DEMs and further calibrated by varying layer densities within a likely range.

Comparing the GPR data to the model results, we found that the GPR data overestimated rock glacier thickness in the upper region of the rock glacier, so we adjusted our "initial guess" propagation velocity in this area. Propagation velocity is likely to vary considerably as a result of changes in composition. This causes significant challenges in the interpretation and processing of the GPR data.

Although significant refinement is necessary and large uncertainties remain, our simple modeling approach was helpful in fine-tuning the analysis of the GPR data, yielding some valuable insights. We believe this method can be applied at other rock glaciers as long as similar assumptions regarding the nature of the rock glacier movement can be made there.

Further geophysical measurements, such as GPR at a range of frequencies, seismic and drilling, would provide additional information about the composition and density of the rock glacier. This would probably be very useful for improving the model from its current status of "one value fits all." Nonetheless, the model results suggest that rock glacier thickness and volume could potentially be estimated from displacement data gained from high-accuracy DEMs for different years, and we find that our simple modeling approach improved the analysis of the GPR data. This could prove useful, particularly in areas where extended fieldwork is impractical.

Acknowledgments

We thank the many people who helped in the field during all measurement campaigns. Special thanks go to Heralt Schneider, Martin Stocker-Waldhuber, Jakob Abermann, and Norbert Span, who were responsible for the velocity measurements and the first GPR campaign, and to Karl Krainer who provided the GPR system. We thank the Austrian Climate and Energy Funds (C4AUSTRIA project, ACRP-A963633), and alpS (MUSICALS project) for supplying the remote sensing data.

This work was supported with a research grant by the University of Innsbruck, Vice Rectorate for Research. We also thank the Alpine Forschungsstelle Obergurgl (AFO) for their support.

Last but not least we would like to express our appreciation for the helpful comments and constructive criticisms made by the reviewers and the associate editor, as well as for their patience.

References Cited

Angillieri, E., and Yanina, M., 2009: A preliminary inventory of rock glaciers at 30° S latitude, Cordillera Frontal of San Juan, Argentina. *Quaternary International,* 195: 151–157.

Arcone, S. A., Lawson, D. E., Delaney, A. J., Strasser, J. C., and Strasser, J. D., 1998: Ground-penetrating radar reflection profiling of groundwater and bedrock in an area of discontinuous permafrost. *Geophysics,* 63: 1573–1584.

Baltsavias, E. P., Favev, E., Bauder, A., Boesch, H., and Pateraki, M., 2001: Digital surface modelling by airborne laser scanning and digital photogrammetry for glacier monitoring. *Photogrammetric Record,* 17(98): 243–273.

Barsch, D., 1977: Alpiner Permafrost—ein Beitrag zur Verbreitung, zum Charakter und zur Ökologie am Beispiel der Schweizer Alpen. *Abhandlungen der Akademie der Wissenschaften.* Göttingen Mathematisch-Physikalische Klasse Folge 3, 31: 118–141.

Barsch, D., 1996: *Rockglaciers: Indicators for the Present and Former Geoecology in High Mountain Environments*. Berlin: Springer-Verlag, Springer Series in Physical Environment, 16.

Barsch, D., and Hell, G., 1975: Photogrammetrische Bewegungsmessungen am Blockgletscher Murtèl I, Oberengadin, Schweizer Alpen. *Zeitschrift für Gletscherkunde und Glazialgeologie*, 11(2): 111–142.

Bauder, A., Funk, M., and Gudmundsson, G. H., 2003: The ice-thickness distribution of Unteraargletscher, Switzerland. *Annals of Glaciology,* 37: 331–336.

Bolch, T., and Marchenko, S., 2009: Significance of glaciers, rockglaciers and ice-rich permafrost in the Northern Tien Shan as water towers under climate change conditions. *In* Braun, L., Hagg, W., Severskiy, I.V., Young, G. J. (eds.), *Selected Papers from the Workshop "Assessment of Snow, Glacier and Water Resources in Asia" held in Almaty, Kazakhstan, 28–30 Nov. [2006]*. Paris, UNESCO-IHP and German National Committee for IHP/HWRP, 179–193.

Bollmann, E., Abermann, J., Klug, C., Sailer, R., and Stötter, J., 2012: Quantifying rockglacier creep using airborne laser scanning a case study from two rockglaciers in the Austrian Alps. *Proceedings of the Tenth International Conference on Permafrost*.

Brenning, A., 2005: Geomorphological, Hydrological and Climatic Significance of Rock Glaciers in the Andes of Central Chile (33–35°S). *Permafrost and Periglacial Processes,* 16: 231–240.

Brenning, A., 2008: The Impact of Mining on Rock Glaciers and Glaciers. *Darkening Peaks: Glacier Retreat, Science, and Society*, 196.

Chaix, A., 1923: Les coulées de blocs du Parc National Suisse d'Engadine (Note préliminaire). *Le Globe*, 62: 1–35.

Cheng, G., and Wu, T., 2007: Responses of permafrost to climate change and their environmental significance, Qinghai-Tibet Plateau. *Journal of Geophysical Research*, 112: F02S03, doi http://dx.doi.org/10.1029/2006JF000631.

Cuffey, K. M., and Paterson, W. S. B., 2010: *The Physics of Glaciers*. Fourth edition. Oxford, U.K.: Elsevier.

Davis, J., and Annan, A., 1989: Ground-penetrating radar for high-resolution mapping of soil and rock stratigraphy. *Geophysical Prospecting,* 37: 531–551.

Degenhardt, J. J., 2009: Developments of tongue-shaped and multilobate rock glaciers in alpine environments—interpretations from ground penetrating radar surveys. *Geomorphology,* 109: 94–107.

Degenhardt, J. J., Giardino, J. R., and Junck, M. B., 2003: GPR survey of a lobate rock glacier in Yankee Boy Basin, Colorado, USA. *Geological Society, London, Special Publications,* 211: 167–179.

Dowdeswell, J. A., and Benham, T. J., 2003: A surge of Perseibreen, Svalbard, examined using aerial photography and ASTER high resolution satellite imagery. *Polar Research*, 22(2): 373–383.

Fukui, K., Sone, T., Strelin, J., Torielli, C., and Mori, J., 2007: Ground penetrating radar sounding on an active rock glacier on James Ross Island, Antarctic Peninsula region. *Polish Polar Research,* 28: 13–22.

Glen, J. W., 1958: The flow law of ice: a discussion of the assumptions made in glacier theory, their experimental foundations and consequences. *IASH Publication*, 47: 171–183.

Glen, J. W., and Paren, J., 1975: The electrical properties of snow and ice. *Journal of Glaciology,* 15: 15–38.

Haeberli, W., and Patzelt, G., 1982: Permafrostkartierung im Gebiet der Hochebenkar-Blockgletscher, Obergurgl, Ötztaler Alpen. *Zeitschrift für Gletscherkunde und Glazialgeologie,* 18: 127–150.

Haeberli, W., Hallet, B., Arenson, L., Elconin, R., Humlum, O., Kääb, A., Kaufmann, V., Ladanyi, B., Matsuoka, N., and Springman, S., 2006: Permafrost creep and rock glacier dynamics. *Permafrost and Periglacial Processes,* 17: 189–214.

Haeberli, W., Noetzli, J., Arenson, L., Delaloye, R., Gärtner-Roer, I., Gruber, S., Isaksen, K., Kneisel, C., Krautblatter, M., and Phillips, M., 2011: Mountain permafrost: development and challenges of a young research field. *Journal of Glaciology*, 56 (200; special issue): 1043–1058.

Hauck, C., and Kneisel, C., 2008: *Applied Geophysics in Periglacial Environments*. Cambridge, U.K.: Cambridge University Press.

Hausmann, H., Krainer, K., Brückl, E, and Mostler, W., 2007: Internal structure and ice content of Reichenkar rock glacier (Stubai Alps, Austria), assessed by geophysical investigations. *Permafrost and Periglacial Processes*, 18: 351–367.

Hausmann, H., Krainer, K., Brückl, E., and Ullrich, C., 2012: Internal structure, ice content and dynamics of Ölgrube and Kaiserberg rock glaciers (Ötztal Alps, Austria) determined from geophysical surveys. *Austrian Journal of Earth Sciences,* 105: 12–31.

Ikeda, A., 2004: *Rock Glacier Dynamics near the Lower Limit of Mountain Permafrost in the Swiss Alps.* Doctoral dissertation, University of Tsukuba, Japan.

Ikeda, A., Matsuoka, N., and Kääb, A., 2008: Fast deformation of perennially frozen debris in a warm rock glacier in the Swiss Alps: an effect of liquid water. *Journal of Geophysical Research*, 113: F01021, doi http://dx.doi.org/10.1029/2007JF000859.

Kääb, A., 2010: Aerial photogrammetry in glacier studies. Pellikka, P., and Rees, W. G. (eds.), *Remote Sensing of Glaciers. Techniques for Topographic, Spatial and Thematic Mapping of Glaciers*. London: Taylor and Francis, 331 pp.

Kääb, A., and Vollmer, M., 2000: Surface geometry, thickness changes and flow fields on permafrost streams: automatic extraction by digital image analysis. *Permafrost and Periglacial Processes,* 8(4): 409–426.

Kääb, A., Gudmundsson, G. H., and Hoelzle, M., 1998: Surface deformation of creeping mountain permafrost. Photogrammetric investigations on rock glacier Murtèl, Swiss Alps. *In* Proceedings, 7th International Conference on Permafrost, Yellowknife, 23–27 June 1998. *Collection Nordicana,* 57: 531–537.

Kääb, A., Isaksen, K., Eiken, T., and Farbrot, H., 2002: Geometry and dynamics of two lobe-shaped rock glaciers in the permafrost of Svalbard. *Norwegian Journal of Geography,* 56: 152–160.

Kääb, A., Kaufmann, V., Ladstädter, R., and Eiken, T., 2003: Rock glacier dynamics: implications from high-resolution measurements of surface velocity fields. *In* Proceedings, Eighth International Conference on Permafrost, 21–25 July, Zurich, Switzerland, 501–506.

Kääb, A., Frauenfelder, R., and Roer, I., 2007: On the response of rockglacier creep to surface temperature increase. *Global and Planetary Change*, 56(1): 172–187.

Kaufmann, V., 2012: The evolution of rock glacier monitoring using terrestrial photogrammetry: the example of Äusseres Hochebenkar rock glacier (Austria). *Austrian Journal of Earth Sciences*, 105(2): 63–77.

Kaufmann, V., and Ladstätter, R., 2002a: Spatio-temporal analysis of the behaviour of the Hochebenkar rock glaciers (Oetztal Alps, Austria) by means of digital photogrammetric methods. *In* Kaufmann, V., and Sulzer, W. (eds.), *Proceedings of the 6th International Symposium on High Mountain Remote Sensing Cartography.* Grazer Schriften der Geographie und Raumforschung, 37, Institute of Geography and Regional Science, University of Graz, 119–139.

Kaufmann, V., and Ladstätter, R., 2002b: Monitoring of active rock glaciers by means of digital photogrammetry. *ISPRS Commission III Symposium*, Graz, IAPRS, 34, 3B, 108–111.

Klug, C., Bollmann, E., Kääb, A., Krainer, K., Sailer, R., and Stötter, J., 2012: Monitoring of permafrost creep on two rock glaciers in the Austrian eastern Alps: combination of aerophotogrammetry and airborne laser scanning. *In* Proceedings, 10th International Conference on Permafrost, Salekhard, Russia, 215–220.

Konrad, S., Humphrey, N., Steig, E., Clark, D., Potter, N., Pfeffer, J., and Pfeffer, W., 1999: Rock glacier dynamics and paleoclimatic implications. *Geology,* 27: 1131–1134.

Kovacs, A., Gow, A. J., and Morey, R. M., 1995: The in-situ dielectric constant of polar firn revisited. *Cold Regions Science and Technology,* 23: 245–256.

Krainer, K., and Ribis, M., 2012: A rock glacier inventory of the Tyrolean Alps (Austria). *Austrian Journal of Earth Sciences*, 105(2): 32–47.

Ladstätter, R., and Kaufmann, V., 2005: Terrestrisch-photogrammetrische Dokumentation des Blockgletschers im Äußeren Hochebenkar. Chesi, G., and Weinold, T. (eds.), *Internationale Geodätische Woche Obergurgl*. Herbert Wichmann Verlag, Heidelberg, 82–101.

Lemke, P., Ren, J., Alley, R. B., Allison, I., Carrasco, J., Flato, G., Fujii, Y., Kaser, G., Mote, P., Thomas, R. H., and Zhang, T., 2007: Observations: changes in snow, ice and frozen ground. *In* Solomon, S., Qin, D., Manning, M., Chen, Z., Marquis, M., Averyt, K. B., Tignor, M., and Miller, H. L. (eds.), *Climate Change 2007: The Physical Science Basis. Contribution of Working Group I to the Fourth Assessment Report of the Intergovernmental Panel on Climate Change*. Cambridge, U.K.: Cambridge University Press.

Maurer, H., and Hauck, C., 2007: Instruments and methods of geophysical imaging of alpine rock glaciers. *Journal of Glaciology,* 53: 110–120.

Narod, B. B., and Clark, G. K., 1994: Miniature high-power impulse transmitter for radio-echo sounding. *Journal of Glaciology*, 40(134): 190–194.

Nickus, U., Abermann, J., Fischer, A., Krainer, K., Schneider, H., Span, N., and Thies, H., 2015: Rock Glacier Äußeres Hochebenkar (Austria)—recent results of a monitoring network. *Zeitschrift für Gletscherkunde und Glazialgeologie*, 47/48: 43–62.

Olyphant, G. A., 1987: Rock glacier response to abrupt changes in talus production. *In* Giardino, J. R., Shroder, J. F., Jr., and Vitek, J. D. (eds.), *Rock Glaciers*. London: Allen and Unwin, 55–64.

Pillewizer, W., 1957: Untersuchungen an Blockströmen der Ötztaler Alpen. *Geomorphologische Abhandlungen des Geographischen Institutes der FU Berlin (Otto-Maul Festschrift),* 5: 163–170.

Rignot, E., Hallet, B., and Fountain, A., 2002: Rock glacier surface motion in Beacon Valley, Antarctica, from Synthetic-Aperture Radar Interferometry. *Geophysical Research Letters*, 29(12): 494–497.

Roer, I., 2005: *Rock Glacier Kinematics in a High Mountain Geosystem*. Ph.D. dissertation. Mathematisch-Naturwissenschaftliche Fakultät, Bonn, Rheinische Friedrich-Wilhelms Universität.

Roer, I., and Nyenhuis, M., 2007: Rockglacier activity studies on a regional scale: comparison of geomorphological mapping and photogrammetric monitoring. *Earth Surface Processes and Landforms,* 32: 1747–1758.

Roer, I., Kääb, A., and Dikau, R., 2005: Rock glacier acceleration in the Turtmann valley (Swiss Alps): probable controls. *Norsk Geografisk Tidsskrift*, 59(2): 157–163.

Scambos, T. A., Dutkiewicz, M. J., Wilson, J. C., and Bindschadler, R. A., 1992: Application of image cross-correlation to the measurement of glacier velocity using satellite image data. *Remote Sensing of Environment*, 42(3): 177–186.

Schallhart, N., and Erschbamer, B. (eds.), 2015: *Forschung am Blockgletscher—Methoden und Ergebnisse.* Alpine Forschungsstelle Obergurgl, Band 4, Innsbruck University Press.

Schneider, B., 1999: *Die Bewegungsmessungen am Blockgletscher im Äußeren Hochebenkar (Ötztaler Alpen, Tirol) seit 1938.* Dissertation, Instituts für Hochgebirgsforschung und Alpenländische Land- und Forstwirtschaft, Universität Innsbruck.

Schneider, B., and Schneider, H., 2001: Zur 60 jährigen Messreihe der kurzfristigen Geschwindigkeitsmessungen am Blockgletscher im Äußeren Hochebenkar, Ötztaler Alpen, Tirol. *Zeitschrift für Gletscherkunde und Glazialgeologie,* 37: 1–33.

Span, N., Fischer, A., Kuhn, M., Massimo, M., and Butschek, M., 2005: Radarmessungen der Eisdicke Österreichischer Gletscher. Band I: Messungen 1995 bis 1998. Österreichische Beiträge zu *Meteorologie und Geophysik*, 33: 13.

Springman, S. M., Arenson, L. U., Yamamoto, Y., Maurer, H., Kos, A., Buchli, T., and Derungs, G., 2012: Multidisciplinary investigations on three rock glaciers in the Swiss Alps:

legacies and future perspectives. *Geographiska Annaler: Series A, Physical Geography*, 94: 215–243.

Vaughan, D. G., Comiso, C. J., Allison, J., Carrasco, J., Kaser, G., Kwok, R., Mote, P., Murray, T., Paul, F., Ren, J., Rignot, E., Solomina, O., Steffen, K., and Zhang, T., 2013: Observations: Cryosphere. Climate Change 2013. *In* Stocker, T. F., et al. (eds.), *The Physical Science Basis. Contribution of Working Group I to the Fifth Assessment Report of the Intergovernmental Panel on Climate Change.* Cambridge, U.K.: Cambridge University Press, 317–382.

Vietoris, L., 1958: Der Blockgletscher des Äußeren Hochebenkars. *Gurgler Berichte 1, Bundessportheim und Alpine Forschungsstelle der Universität Innsbruck, Obergurgl*, 41–45.

Vietoris, L., 1972: Über den Blockgletscher des Äußeren Hochebenkars. *Zeitschrift für Gletscherkunde und Glazialgeologie,* 8: 169–188.

Von Der Mühl, D., Hauck, C., and Gubler, H., 2002: Mapping of mountain permafrost using geophysical methods. *Progress in Physical Geography,* 26: 643–660.

MS submitted 25 October 2014
MS accepted 28 January 2016